Artificial
Organs

Starling-Like Flow Control of a Left Ventricular Assist Device: In Vitro Validation

*Nicholas R. Gaddum, †‡Michael Stevens, §Einly Lim, ‡John Fraser, §Nigel Lovell, †David Mason, ¶Daniel Timms, and **††Robert Salamonsen

**Division of Imaging Sciences and Biomedical Engineering, St. Thomas' Hospital, King's College London, London, UK; †School of Information Technology and Electrical Engineering, University of Queensland; ‡Critical Care Research Group, Intensive Care Unit, The Prince Charles Hospital, and University of Queensland, Brisbane, Queensland; §Graduate School of Biomedical Engineering, University of New South Wales, Sydney, New South Wales; **Department of Epidemiology and Preventative Medicine, University of Monash; ††Intensive Care Unit, Alfred Hospital, Melbourne, Victoria, Australia; and ¶Center for Technology Innovation, Texas Heart Institute, Houston, TX, USA*

Abstract: The application of rotary left ventricular (LV) assist devices (LVADs) is expanding from bridge to transplant, to destination and bridge to recovery therapy. Conventional constant speed LVAD controllers do not regulate flow according to preload, and can cause over/underpumping, leading to harmful ventricular suction or pulmonary edema, respectively. We implemented a novel adaptive controller which maintains a linear relationship between mean flow and flow pulsatility to imitate native Starling-like flow regulation which requires only the measurement of VAD flow. In vitro controller evaluation was conducted and the flow sensitivity was compared during simulations of postural change, pulmonary hypertension, and the transition from sleep to wake. The Starling-like controller's flow sensitivity to preload was measured as 0.39 L/min/mm Hg, 10 times greater than constant speed control (0.04 L/min/mm Hg). Constant speed control induced LV suction after sudden simulated pulmonary hypertension, whereas Starling-like control reduced mean flow from 4.14 to 3.58 L/min, maintaining safe support. From simulated sleep to wake, Starling-like control increased flow 2.93 to 4.11 L/min as a response to the increased residual LV pulsatility. The proposed controller has the potential to better match device outflow to patient demand in comparison with conventional constant speed control. **Key Words:** Left ventricular assist device control—Heart failure—Pulsatility index—Flow control—Frank–Starling mechanism.

Rotary ventricular assist devices (VADs) now have a well-established place in the medical management of severe left ventricular (LV) failure supporting patients indefinitely, or until recovery or transplant (1). Despite their smaller size, higher durability, and lower power consumption over positive displacement devices, they do not have the ability of the natural ventricles to control blood flow when operated in the conventional constant speed mode of control (2).

The natural ventricles synchronize outputs by augmenting the force of contraction as the ventricular filling pressure (preload) increases. This mechanism was sequentially expanded after initial pressure measurement by Coats in 1869 (3), to pressure and volume measurements by Frank in 1895 (4), to pressure and flow measurements by Starling and Visscher in 1926 (5). Commonly referred to as the Frank–Starling (6) mechanism, it describes the regulation of stroke volume (and therefore arterial flow) according to the rate of venous blood returning to the ventricles (venous return). The native ventricle's preload sensitivity is dependent on inotropy and has been documented as high as 4 L/min/mm Hg in normal subjects (7) and as low as around 0.2 L/min/mm Hg in a cohort of patients with "minimally compromised" left ventricular contractility (2). This sensitivity is responsible for a 24% diurnal variation in cardiac output in healthy subjects (8), and permits a flow range from 5.3 to 15.2 L/min during exercise (9). Rotary pumps provide positive flow and a pressure

doi:10.1111/aor.12221

Received June 2013; revised August 2013.

Address correspondence and reprint requests to Dr. Nicholas R. Gaddum, Imaging Sciences, 4th Floor Lambeth Wing, St. Thomas' Hospital, London, SE17EH, UK. E-mail: nickgaddum@gmail.com

potential which "floats" above the inlet pressure, determined by the characteristic pump performance given to pump speed and vascular resistance (10). During support, magnitudes of preload fluctuation are considerably outweighed by arterial pressure variation caused by, for example, changes in systemic resistance. This makes their function "unphysiological" when compared with the native heart (2).

Various LVAD controllers have been introduced, including those which maintain constant flow (11), arterial pressure (12), pressure head across the VAD (13), or match peak ventricular systolic and arterial pressures (14). Although these controllers are physiologically responsive, flow through the pump ideally should be sensitive to preload in order to prevent suction events and respond to increased demand during low-level exercise. Theoretically, if both the flow and preload are accurately measured during VAD support, then native flow control could be emulated (15) to provide safe and robust ventricular support for VAD patients.

Measuring VAD flow has been achieved either using a flow sensor incorporated into the pumping system (16), or in sensorless configurations through observation of power and speed signals (17) and estimation of blood viscosity (18).

Far more complicated is the measurement of preload, as thrombus build-up on the pressure sensor and signal drift (19) prevents the use of currently available implantable sensors in long-term VAD control. Passive VAD control systems have been proposed, such as flexible pump geometries, where the efficiency (and therefore output) of the pump is affected by the surrounding blood pressure (20,21). However, the overbearing influence of arterial pressure reduced sensitivity to inlet pressure. Flexible inlet cannulae have also been used to throttle flow out of the ventricle as inlet pressure decreases (22). Although able to reduce flow near suction, flow sensitivity to increasing preload was not achieved.

Finally, with access only to reliable flow measurement, physiological control is complicated further by the need for adaptive support to account for diurnal metabolic demand (varying inotropy) and varying patient sizes.

Salamonsen et al. proposed a Starling-like VAD controller which emulates the native flow sensitivity to preload of the natural LV (23). They noted that not only the relationship between cardiac output and preload was sigmoid-like in form (7), but also the relationship between aortic flow pulsatility and preload was similarly sigmoid shaped. As a consequence, the Starling characteristic relating pump flow to pulsatility is approximately linear. This offers a means of imitating native flow sensitivity to preload in a VAD with only a flow signal. An adaptive control strategy was also described where the gradient of the linear controller line could be increased or decreased when VAD operation extended outside preset maximum/minimum limits of both pump flow and flow pulsatility (23). Although the novel features of this control mode were described in detail, the technique was not assessed and validated in a realistic circulatory simulation. The aim of this study, therefore, was to implement the Starling-like controller in vitro to characterize the Starling-like flow sensitivity to preload, and compare its operation with that of a standard constant speed VAD controller.

BACKGROUND

Starling-like control

Salamonsen et al. proposed that Starling-like flow sensitivity to preload would be achieved if a linear relationship between flow and flow pulsatility could be maintained (23). In this case, flow pulsatility (ΔQ) was defined as the amplitude of the flow profile through the VAD as illustrated in Fig. 1, left. The rotary VAD is operated such that the operating point (mean flow, flow pulsatility) operates only on a straight line when represented on flow versus flow pulsatility axes. This straight line will be referred to as the "control line." For example (see Case A in Fig. 1, center), let point A be the current operation point of a VAD during support, with the Starling-like controller maintaining pump operation on a control line at an angle of $\theta = 55°$ to the horizontal flow pulsatility axis. If some disturbance changes the cardiovascular (CV) system state in any way (lying down, sleep, waking activity, etc.), the operation point may deviate from the control line. The controller then modulates the pump rotational speed to restore the operation point at a new position (point B) back on the control line. This is analogous to moving back and forward along Starling's sigmoid-shaped arterial flow versus preload relationship.

To accommodate different patient sizes, changes in venous return during sleep/waking activity or to respond to an improving trans-pulmonary gradient, the control strategy needs to be adaptive. Starling's law accommodates such changes by magnifying the sigmoid-shaped arterial flow versus preload relationships along the vertical arterial flow axis (7).

Consider a patient changing from a sleeping to a more active waking state during Starling-like controlled VAD support. Adaptive control in this case needs to increase the control line angle to compensate for an increased venous return after initial

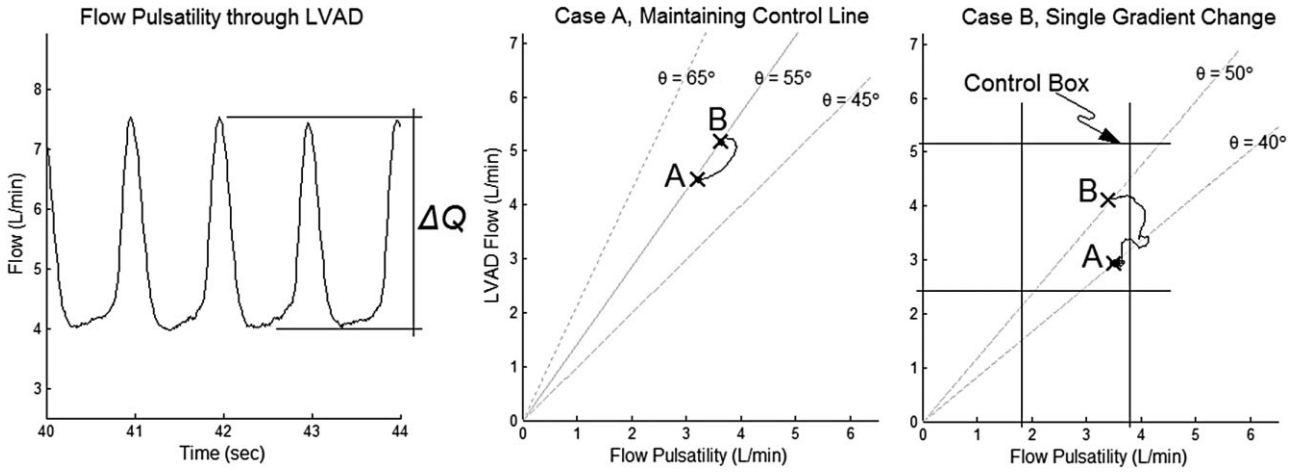

FIG. 1. Illustrated definition of flow pulsatility through LVAD (left), Starling-like controller maintaining pump operation upon a control line of angle $\theta = 55°$ (center, Case A), adaptation of control line gradient from $\theta = 40°$ to 50° following sleep to waking (right, Case B).

muscular activity. We propose the trigger for such adaptation is a predefined "control box," defined by upper and lower limits of flow and flow pulsatility (see Case B in Fig. 1, right). The control box defines a region within which VAD operation points can reside, and outside which they should not. In this right-hand plot, the VAD is originally operating upon a control line with $\theta = 40°$ at operating point A. As the patient wakes, and blood CO_2 levels elevate, vessels dilate, causing an increased venous return and thus residual LV function is increased. At this point, the pulsatility rises above a preset threshold of (in this case) 3.7 L/min. The adaptive controller increases the control line angle to $\theta = 50°$, and the pump speed is subsequently modulated to drive the operating point up to the new control line, point B. The response time and excursion path between points A and B are dictated by the definition of the operating point error, in silico controller parameters, and their interaction with the CV system itself.

METHODS

In vitro simulation

Simulations were carried out in an experimental, PC controlled mock circulation loop (MCL) incorporating both systemic and pulmonary circuits connected in series (see Fig. 2). Active control of vascular resistance, contractility, and systemic venous compliance (SVC) permitted repeatable simulation of CV system perturbations to observe device/circulation interaction. Further detail of the MCL operation can be found in Timms et al. (24). All MCL operational and control software was written in MATLAB (The MathWorks, Natick, MA, USA).

Although all tests simulated LV support during depressed LV function, residual function was generated by the PC-controlled ventricle in accordance with a scaled Starling-like relationship. This relationship was recreated through measurement of preload and LV end diastolic volume, and subsequent active control of the ventricle contractility (25). The MCL was operated at 60 bpm, with a working fluid of 40% (by weight) glycerol–water solution to simulate blood viscosity. All sensor signals were sampled, and LVAD motor, pneumatic ventricles, and venous

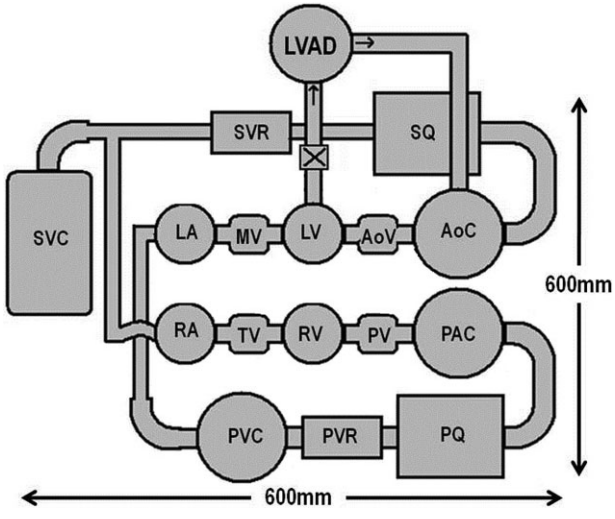

FIG. 2. Schematic of the dual circuit MCL; LA, left atrium; MV, mitral valve; LV, left ventricle; AoV, aortic valve; AoC, systemic arterial compliance; SQ, systemic flow meter; SVR, systemic venous resistance; RA, right atrium; TV, tricuspid valve; RV, right ventricle; PV, pulmonary valve; PAC, pulmonary arterial compliance; PQ, pulmonary flow meter; PVR, pulmonary venous resistance; PVC, pulmonary venous compliance; SVC, systemic venous compliance.

resistance were actuated, at 2 kHz. A VentrAssist LVAD (VentraCor, Sydney, Australia) was used to support the simulated failing LV in the MCL. The LVAD cannulated the LV and the aorta (aortic compliance chamber).

Control algorithm

Although the VentrAssist normally derives flow (Q) from power signals to the LVAD (17), flow was directly measured at the outlet cannula using a gold-standard ultrasound cuff (TS402-10PXL, Transonic Systems, Ithaca, NY, USA). Pump speed (N) was inferred via the back electromotive force measurement generated by the VentrAssist motor coils. Tighter proportional integral and derivative (PID) speed control than provided by the clinical VentrAssist controller was implemented via direct control of the duty cycle of the pulse width modulation (PWM) signal to the LVAD motor coils. Starling-like control was actuated in a two-step control chain (see Fig. 3). From the flow signal, retrospective mean flow (Q_M) and flow pulsatility (ΔQ) measurements allowed the operation point to be located with respect to the control box (see Fig. 1). The flow pulsatility was defined as the time-averaged amplitude of the flow signal at the end of every complete cardiac cycle. Q_M was obtained using the nonlinear morphological filter in order to obtain an accurate, responsive, and pulse-free signal (26).

A conditional statement then determined whether the operation point (Q_M, ΔQ) was within the control box. Provided the conditional statement was satisfied, a mean flow error (Q_{error}) was evaluated based on the difference between the current flow and a measured target flow (Q_{Target}). In this study, two different errors were defined by two different descriptions of Q_{Target}. The first, Vertical Error, defined the target flow as a vertical projection from the current flow pulsatility to the control line. The second, Radial Error, defined the target flow from a tangential projection about the Q_M, ΔQ origin toward the control line. Finally, Q_{error} is fed into a flow PID controller to modulate the duty cycle of the PWM signal and so drive the operating point toward the target flow, and therefore coincident with the control line. The PID controller used a tolerance of 2% for Q_{error} to reduce unnecessary small changes in pump speed.

If the initial conditional statement was not satisfied and the operating point was outside the control box, then a timer began counting the number of time steps that the operation point remained outside. If the timer exceeded some preset limit ($Timer1_{MAX}$, set at 10 s), then the adaptive controller adjusted the angle of the control line as illustrated in Fig. 1, center. If the operation point remained outside the control box despite changes in control line angle and the timer exceeded a second greater limit ($Timer2_{MAX}$), then an alarm was initiated for a clinician to intervene (i.e., add/remove intravenous fluid). This latter alarm feature of the controller was not incorporated into this study.

System lines

In order to understand how the CV system responds to a flow and flow pulsatility coordinate system during various system perturbations, the first tests were designed to define characteristic "system lines." To do this, various system parameters were varied during Starling-like control of LVAD support. For each parametric variation, the control line angle was incrementally increased over a range within the physical limits of the MCL (minimum/maximum

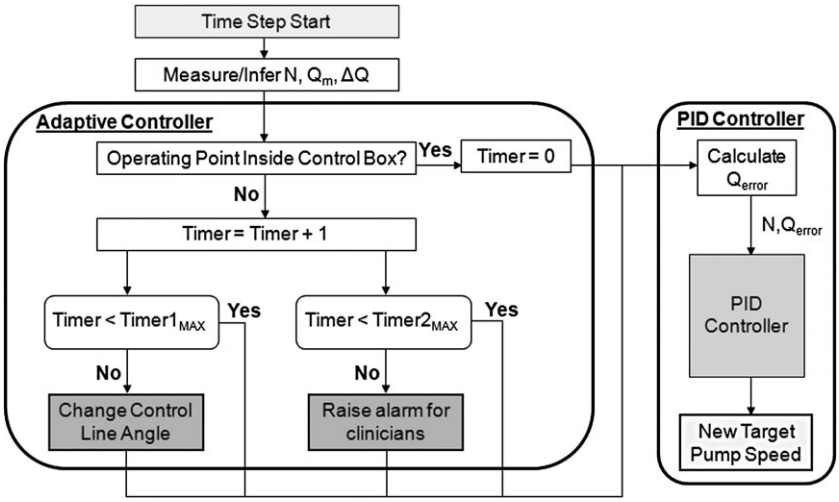

FIG. 3. Schematic of adaptive and proportional integral and derivative (PID) controllers which together constitute the Starling-like rotary VAD controller; N, rotational speed; Q, flow; ΔQ, flow pulsatility; Timer, cumulative time steps where the operation point has stayed outside the control box; $Timer1_{MAX}$, preset Timer limit before the control line angle is changed; $Timer2_{MAX}$, preset Timer limit before it is assumed clinical intervention is required.

angle $\theta = 15/65°$, respectively). Varied parameters included systemic resistance (1000 to 1600 Dynes), central venous pressure (CVP, 6 to 10 mm Hg), LV contractility (generic; low to high), and LV systolic time (45 to 75% of the cardiac cycle). Default parameters for these tests (when not being varied) were CVP = 8 mm Hg, LV contractility = medium, and LV systolic time = 45%. During each test, the control line angle was initiated at the lowest possible angle, and the system was allowed to settle to a steady state. Then the angle was increased by increments of 10°, allowing the system to reach a steady state after each increment. The resulting "system lines" describe the behavior of steady-state physiology in terms of Q_M versus ΔQ profiles, where only pump speed is varied.

Starling-like control

Comparisons between the proposed Starling-like and constant speed VAD controller were made by subjecting each controller to simulations of three sudden hemodynamic perturbations. Left atrial pressure (LAP) and systemic flow are considered along with the pump speed before, during, and after the perturbations. The flow sensitivity to preload was also assessed as a measure of "Starling-like" behavior.

The first test simulates a supported patient moving from a standing position to a lying position; the second simulates sudden pulmonary hypertension during LVAD support, such as experienced during a Valsalva maneuver. Both of these simulations assume that the control box is wide enough that the control line gradient is not changed; therefore PID control, and no adaptive control (see Fig. 3). The third simulates a two-stage change of system state from sleep to waking activity. This final case sees changes in control line gradient in order to retain the operation point within the preset control box; therefore, PID control and adaptive control.

To simulate sudden lying down, stable LV support was initiated for both the Starling-like controller and constant speed controller with a mean aortic pressure (AoP) of around 90 mm Hg and mean systemic flow of 4.5 L/min. Lying down was simulated by forcing systemic venous fluid into the circulation by injecting compressed air into the top of the SVC chamber (see Fig. 2). The control line angle was initiated at $\theta = 55°$.

Simulating sudden pulmonary hypertension during support was initiated again with a flow around 4 L/min, and AoPs around 90 mm Hg. Pulmonary hypertension was simulated with a sudden increase in pulmonary vascular resistance. The control line angle was set at $\theta = 50°$.

The simulation of sleep to wake activity required the variation of both contractility and systemic resistance to simulate inotropy and dilation of resistance vessels in the muscles. Initially, depressed hemodynamics during simulated sleep were set around 3 L/min and 85 mm Hg, supported with an initial control line at $\theta = 40°$. The control box was defined by upper and lower mean flow and flow pulsatility limits of $Q_M = 7.0$ and 2.0 L/min, $\Delta Q = 3.7$ and 0.7 L/min, respectively. A sudden increase in left and right ventricular contractility and decrease in systemic resistance simulated this transition as human metabolic demand starts to increase.

The first perturbation simulation (lying down) was also used to compare the radial and the vertical error assessments. In order to compare two experimental responses, comparisons were made between normalized excursions from an initial operating point (Q_M, ΔQ coordinate) before the perturbation ($t = t_A$), until the operating point after a new steady state ($t = t_B$) was reached (from A to B [crosses], see Fig. 5 center). A retrospective error ($E_R(t)$) profile based on the final steady-state operating point ($Q_{M,B}$, ΔQ_B) was calculated for each of the two error definitions. This was defined as,

$$E_R(t) = \frac{1}{f}\sqrt{(\boldsymbol{Q_{M,B}} - \boldsymbol{Q_M(t)})^2 + (\Delta \boldsymbol{Q_B} - \Delta \boldsymbol{Q(t)})^2},$$

where bold characters represent normalized variables. Two measures of both errors' efficacies were calculated. The first was the rise time, calculated as the time from point A before the E_R settled below 10%. The second was the cumulative sum of the vertical or radial $E_R(t)$ profiles.

All the sudden changes in hemodynamics (e.g., resistance/contractility) were actively controlled using the MCL operational software. This permitted disturbances to be as repeatable as reasonably possible between compared experimental simulations.

RESULTS

System lines

Figure 4 indicates the orientation and position of the system lines as various physiological parameters are changed. As the control angle was increased throughout this test, the PID controller would increase pump speed in order to reduce flow pulsatility, and increase flow. Subsequently, the LV was incrementally unloaded causing the MCL Starling control of the pneumatic ventricles to decrease the contractility, and therefore the flow pulsatility through the LVAD. Therefore, the system state lines had a negative gradient as the control line

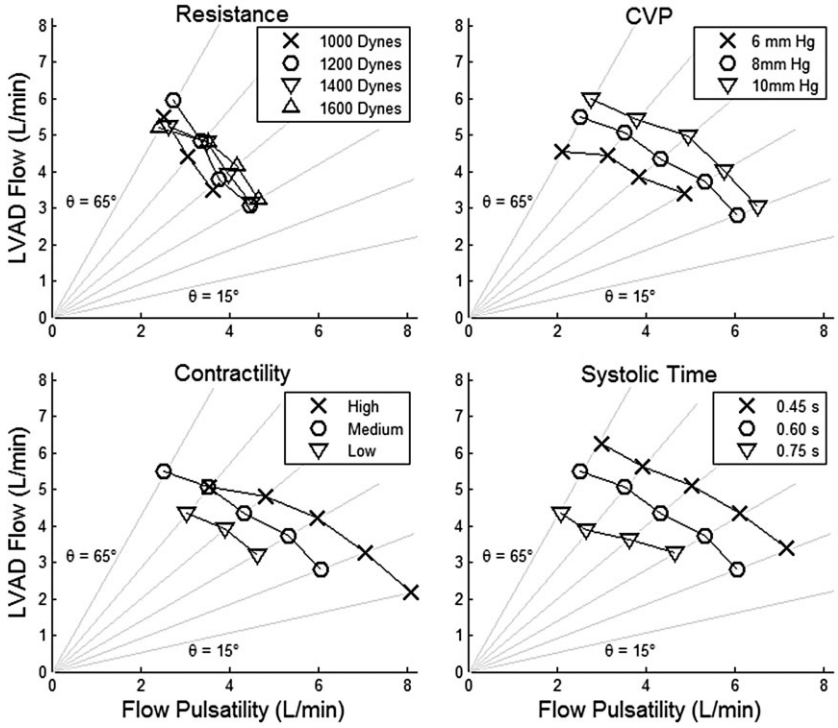

FIG. 4. Exploration of "system lines" of the supported circulation affected by variations in systemic resistance (top left), central venous pressure (top right), LV contractility (bottom left), and systolic time (bottom right), while manually changing the control line gradient.

angle increased, forming an arc centered approximately at the origin.

As resistance, CVP, and contractility were increased, and as the systolic time decreased, the system line would move further from the origin. Resistance increases had the least impact on moving the system line. CVP, contractility, and systolic time, however, had a stronger influence on the radius of the system line arc.

Starling-like control

Figures 5–7 provide side-by-side comparisons of the interactions between the CV system and both the Starling-like controller and the constant speed controller. LAP, peak systolic left ventricular pressure (Sys. LVP), and AoP are indicated for each controller in the left and right plots, respectively. The central plots in each of these figures show the movement of the operating point about the Q_M versus ΔQ axes for both controllers. In these plots, the steady-state operating points before and after each simulated perturbation are given (points A, B, etc.).

Figure 5 presents the simulations during a standing to lying maneuver with Starling-like controllers based on radial error (black cross marker), vertical error (gray cross marker), and a constant speed controller (gray plus marker). Simulated lying forced systemic venous fluid into the right atrium, causing the characteristic right ventricle Starling response of the MCL to increase pulmonary flow. Subsequently, LV preload was sharply increased, resulting in the characteristic left ventricular Starling response of the MCL to increase residual left ventricular contractile function and therefore increasing ΔQ through the VAD to increase (see Table 1).

Employing a radial error permitted a lower rise time and lower retrospective error than using the vertical error alone (42.75 s and 19.96 L/min/s compared with 51.90 s and 28.43 L/min/s, respectively). Thus, the radial error was used for all subsequent simulations.

Comparing the controller responses, the Starling-like controller (with radial error) elevated the LVAD speed due to the increase in preload, and subsequent LV-induced flow pulsatility. The PID controller then returned the operation point to the $\theta = 55°$ control line, increasing flow from 4.48 to 5.17 L/min due to the change of system line caused by an increase in CVP. The apparent preload sensitivity of the Starling-like controller was 0.39 L/min/mm Hg after the sudden destabilization (see Table 1). The constant speed controller maintained speed, and observed a small increase in flow from 4.67 to 4.81 L/min caused by the rotary pump's low, yet inherent preload sensitivity (0.04 L/min/mm Hg).

Simulated pulmonary hypertension in Fig. 6 shows the Starling-like controller's ability to evade suction with a sudden reduction of pulmonary venous return

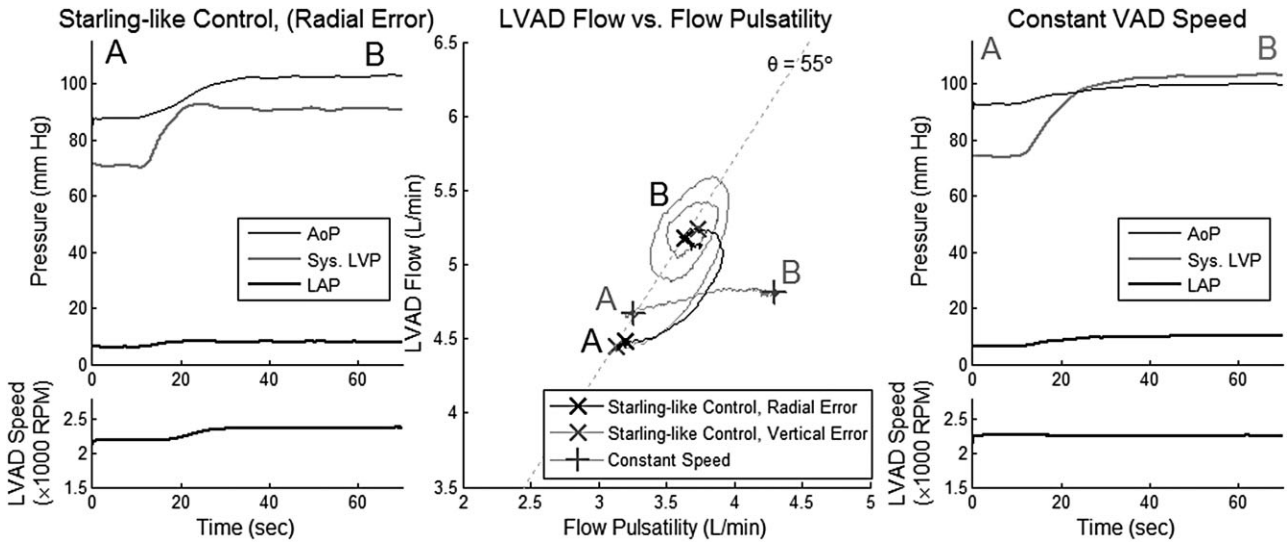

FIG. 5. LVAD support using Starling-like control (left and center) versus constant speed control (right and center) during sudden simulated lying down. A Starling-like controller employing a radial error (black cross marker) is compared with the same controller employing a vertical error (gray cross marker) (center), on the Q_M versus ΔQ axes. The constant speed controller response is shown on the same axes (gray plus marker). Hemodynamic plots of left heart and systemic pressures on the left and right are affected by the sudden lying down at 10 s. The central plot of LVAD flow versus flow pulsatility shows the operating points before and after the destabilization (A and B).

to the LV. Sudden reduction in venous return decreased LAP and subsequently ΔQ. The Starling-like controller responded by decreasing LVAD speed in order to return the operation point back to the control line (A to B [black]). Consequently, flow is reduced from 4.14 to 3.58 L/min to account for the drop in LV preload. The constant speed controller, however, rapidly evacuated the LV of blood, causing suction at around 15 s. The MCL does not accurately simulate hemodynamics following suction. For this reason, the presented hemodynamic data following the point of suction should be ignored.

Simulated sleep, followed by waking activity, is presented in Fig. 7. The flow versus flow pulsatility plot for the Starling-like controller is also presented with the control box in Fig. 1 (right). At 10 s, the flow

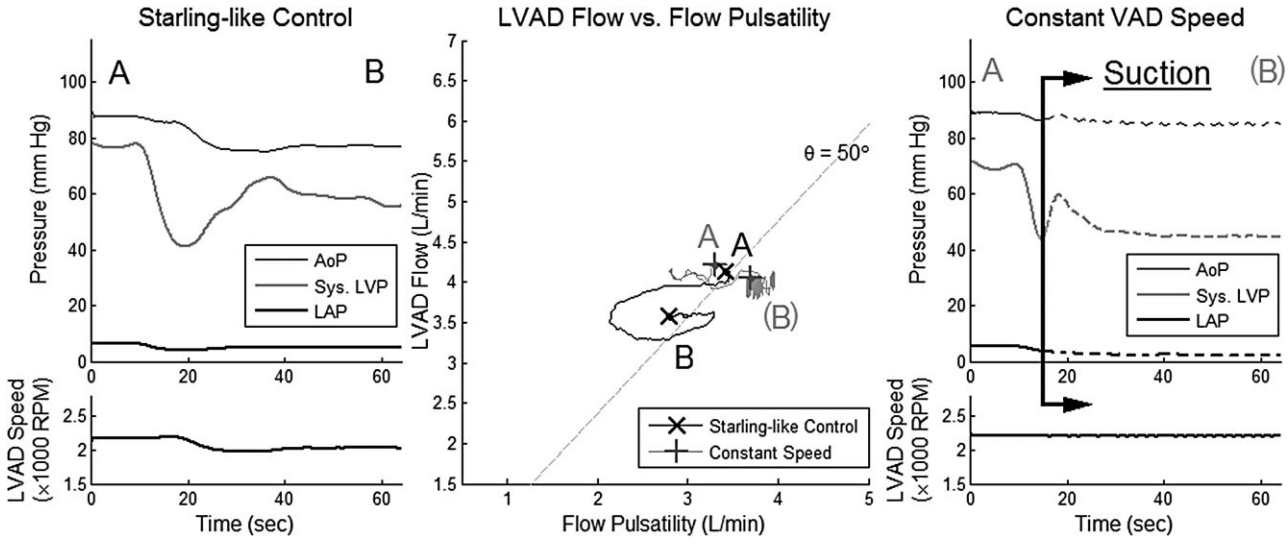

FIG. 6. LVAD support using Starling-like control (left and center) versus constant speed control (right and center) during sudden simulated pulmonary hypertension. Hemodynamic plots of left heart and systemic pressures on the left and right are affected by the sudden hypertension at 10 s. The central plot of LVAD flow versus flow pulsatility shows the operating points before and after the destabilization (A and B).

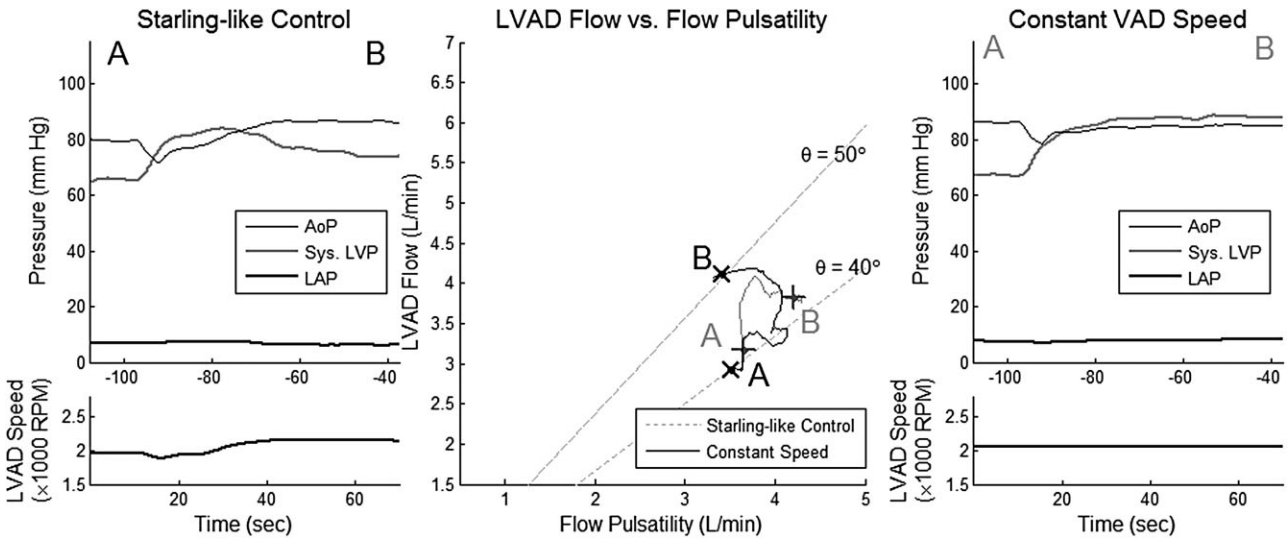

FIG. 7. LVAD support using Starling-like control (left and center) versus constant speed control (right and center) during simulated sleep to waking activity. Hemodynamic plots of left heart and systemic pressures on the left and right are affected by waking at around 10 s. The central plot of LVAD flow versus flow pulsatility shows the operating points before and after the destabilization; A to B, sleep to wake (controller gradient θ = 40° to 50°).

pulsatility increased due to an increase in ventricular contractility. Consequently, the Starling-like controller increases speed to increase flow in order to migrate up the control lines. Upon passing the upper flow pulsatility limit of 3.7 L/min, the control line angle is increased from θ = 40 to 50°.

During constant speed control, flow is increased from 3.2 L/min to just over 3.8 L/min from sleep to waking. Based on results in Figs. 5 and 6 where very little preload flow sensitivity was observed, it appears as though this flow increase was probably due to increased inotropy. Nevertheless, the increase in flow is a total of 0.62 L/min, as opposed to the Starling-like controller which observed a flow increase of almost twice this, 1.18 L/min (see Table 1).

Table 1 shows the controller comparison parameters for the radial and vertical errors. Additionally, the raw Q_M, ΔQ, LAP, and flow sensitivity to preload (preload sensitivity) data are provided for each of the three physiological pertubation tests for both the Starling-like controller and the constant speed controller. At control line gradients of θ = 55° and 50°, pre-load flow sensitivity of the Starling-like controller was 0.39 and 0.33 L/min/mm Hg, respectively. This sensitivity was almost 10 times that of the rotary LVAD's inherent flow sensitivity when operated at constant speed (0.04 L/min/mm Hg) during the lie down simulation. The results for the constant speed controller in brackets during hypertension indicate that these were after suction, and therefore not accurately simulated with the MCL. The sleep to wake preload sensitivities have been omitted as the ventricular function changed (contractility increases); therefore, changes in flow were not only attributed to the LVAD.

DISCUSSION

The efficacy of the Starling-like flow controller is based on sigmoid relationships between both Starling's arterial flow versus preload relationship, and flow pulsatility versus preload (23). Substituting for preload therefore provides a convenient linear relationship between flow and flow pulsatility, requiring only a flow measurement (i.e., without the need for blood immersed pressure sensors), to imitate the Frank–Starling mechanism. This study presents the characterization and implementation of the controller in vitro to validate the flow sensitivity to preload and compare it with conventional constant speed control.

We implemented the Starling-like controller with a two-part controller structure. The initial adaptive controller observes the operation point with respect to a preset control box in order to change control line angle, or to raise an alarm. A secondary PID controller maintains the operation point on the control line by modulating the pump speed.

System lines

"System lines" indicate a path of unchanging CV physiology as the pump speed is increased upon the Q_M versus ΔQ coordinate system. These system lines were explored in an attempt to understand how

TABLE 1. *Raw quantification of flow sensitivity to preload changes*

		Radial error				Vertical error				
Rise time (s)		42.75				51.90				
Cumulative retrospective error (L/min/s)		19.96				28.43				
		Starling-like controller				Constant speed controller				
		ΔQ (L/min)	LAP (mm Hg)	Q_M (L/min)	Preload sensitivity (L/min/mm Hg)	ΔQ (L/min)	LAP (mm Hg)	Q_M (L/min)	Preload sensitivity (L/min/mm Hg)	
Lie down	A	3.20	6.20	4.48	0.39	3.26	6.31	4.67	0.04	
	B	3.64	7.96	5.17		4.30	9.95	4.81		
Pulmonary hypertension	A	3.42	4.87	3.58	0.33	3.30	5.39	4.22	(0.05)	
	B	2.80	6.56	4.14		(3.70)	(2.20)	(4.05)		
Sleep to wake	A	3.50	6.61	2.93	n/a	3.60	7.38	3.18	n/a	
	B	3.40	6.22	4.11		4.27	7.96	3.80		

Numbers in parentheses are nonrepresentative measurements as measured during ventricular suction.
n/a, not applicable.

stable physiology is represented in such coordinates. Generally, these can be described as arcs centered at the origin, and the arc radius increases with increasing vascular resistance, CVP, contractility, and decreasing systolic time. Similarly, one would expect that other changes in the physiology would also increase/decrease the radius of the system arc around the radius: heart rate, exercise, respiratory maneuvers (Valsalva/Mueller), etc. In essence, if preload is reduced or afterload increased, then pulsatility and flow will decrease, reducing the arc radius. If the preload increased or afterload decreased, then pulsatility and flow will increase, increasing the arc radius.

For Starling-like control, a control line at a defined gradient is selected, and pump speed is controlled to maintain the support operating point at its intersection with the arc-shaped "system line." The importance of this concept is that provided there is a unique control gradient, and the physiology is at steady state, there is one unique operation point. Thus, if there is any change in physiology (such as those presented), the controller needs to modulate the pump speed in order to locate the new unique operation point for the new "system line."

Starling-like control

Given that these system lines have an arc profile about the Q_M versus ΔQ axes, it is not surprising that a similarly orientated radial error offered a faster rise time and lower cumulative retrospective error than a vertical error. However, it should be noted that these controller error measures are also determined by the latent response of the MCL to redistribute the working fluid, which may be different between patients.

On top of implementation in vitro, the aim of this study was to characterize this controller's flow sensitivity to preload, and compare its operation with a standard constant speed VAD controller. The Starling-like controller's flow sensitivity to preload, like the native heart, is dependent on demand. As the control line gradient increases, so, too, does sensitivity. This was illustrated in Figs. 5 and 6, where gradients of $\theta = 50°$ and 55° resulted in sensitivities of 0.33 and 0.39 L/min/mm Hg, respectively. The way that control line gradient relates to flow sensitivity to preload, however, will vary between patients. This will depend on the residual function of their supported LVs, in particular how their left atrial pressure relates to their flow pulsatility.

Employing constant speed control, any flow sensitivity to preload will be dependent on the inherent sensitivity of the VAD and cannulae configuration,

which depends on the VAD pump performance curve gradient (25), and the cannulae resistance (15). Regardless, for a rotary pump at fixed speed this sensitivity is low. In this study, the flow sensitivity to preload during constant speed was 0.04 L/min/mm Hg. This low inherent flow sensitivity to preload is similar to those reported for other LVADs (2).

A comparison of flow sensitivity to preload between the Starling-like and constant speed controller is plainly illustrated in Fig. 5. The sudden physiological response to lying down results in an acute increase in CVP, thus moving the system line arc away from the Q_M versus ΔQ origin. When operating at constant speed, pulsatility (and preload) increases and so the new unique operation point (given a flow sensitivity to preload of 0.04 L/min/mm Hg) sees a fractional increase of flow. The Starling-like controller, however, modulates the pump speed to drive the operation point to the intersection of the 55° control line and the new system line, inducing a substantially higher flow sensitivity to preload of 0.39 L/min/mm Hg.

Figure 6 shows the Starling-like controller naturally avoiding suction by reducing flow from 4.14 to 3.58 L/min to account for the reduced venous return. With the same physiological perturbation, the constant speed causes LV volume to decline due to the mismatch between venous return and evacuating LVAD flow. LV suction occurs shortly after.

Beyond the Starling-like controller's ability to simulate a single sigmoid-shaped Starling flow control curve, an adaptive feature was added through the application of a control box. Upper and lower limits for both Q_M and ΔQ, along with $Timer1_{MAX}$ monitored the operation point to assess any necessary changes in control gradient, just as the native heart changes inotropy. This concept was illustrated through simulated sleep to waking activity. During sleep, cardiac output is depressed. Following waking and low level activity, the native sigmoid-shaped relationship between preload and cardiac output is effectively scaled to provide a higher flow sensitivity to preload (7). The Starling-like controller observed two changes in control line gradient ($\theta = 40$ to 50°), as the upper limit of ΔQ was repeatedly reached. Consequently, the flow sensitivity to preload increased as the gradient increased. Comparing this to the constant speed control, increases in flow are observed although this was due to simulated increases in venous return and contractility, thus were induced primarily by increased residual LV function.

Subsequent preclinical trials are needed to develop the adaptive aspect of this controller to (i) assess the time delay between LVAD speed changes and pulmonary venous pressure changes (i.e., $Timer1_{MAX}$); (ii) determine suitable gradient intervals; (iii) select PID controller parameters; and (iv) determine reasonable control box limits.

Limitations

The primary issue with the proposed Starling-like controller is that only flow through the LVAD is considered. Any systemic flow through the aortic valve should ideally be quantified in combination with LVAD flow to correctly determine the operation point. This was not an issue with the presented Starling-like controller simulations as the aortic valve was not opening during steady-state operation. Nevertheless, as VAD applications extend toward recovery (27), it is important that the aortic valve be allowed/encouraged to open. Our group has developed observers for the opening of the aortic valve (28) which will in time be incorporated into the Starling-like control strategy. However, quantifying aortic valve flow remains a challenge.

Another important issue of pulsatility-based flow control is that some residual ventricular function is needed. If this function is lost, then ΔQ will drop, causing the pump speed to reduce Q_M, drawing the operation point down toward the origin. However, eventually the operation point will cross both the Q_M and ΔQ minima, to reside in the lower left quadrant of the controller plot. As described previously, this region, along with the upper right quadrant, cannot be corrected by the LVAD controller and will signal an alarm for intervention by clinical manager of the patient (23).

Although the Starling-like controller increased flow sensitivity to preload, when compared with a constant speed controller (0.39 vs. 0.04 L/min/mm Hg respectively), this is still substantially lower than the maximum native heart's maximum flow sensitivity to flow reported by Guyton and Hall, 4 L/min/mm Hg (7). As stated, increasing the control line gradient will increase the Starling-like controller's inherent flow sensitivity to preload; however, this may be affected by impedance to pulsatile flow caused by long and low diameter cannulae. Reducing the total parallel circuit length and using wide cannulae may allow the pump to better relate the observed pulsatility to the actual LV preload.

Little detail has been presented regarding the linear PID control parameters used to maintain the operation point on the control line. Primarily, this is due to limitations in the accuracy of the MCL to simulate global cardiovascular physiology. We envisage that for optimal adaptive control, the proportional, integral, and differential constants also need to

be adaptive. The adaptive nature of these parameters should be based on the dynamic path of the operating point's excursions between steady states, as well as traditional measures of controller performance such as rise time, overshoot, and integrated error. This work is ongoing in preparation for the preclinical evaluation of the Starling-like controller.

CONCLUSION

An adaptive Starling-like left ventricular assist device control strategy was implemented in vitro and characterized using comparisons to standard constant speed control. The sigmoid-shaped Starling flow sensitivity to preload was imitated with a linear LVAD control line upon flow pulsatility (ΔQ) versus flow (Q_M) axes. Starling-like control evaded suction during sudden simulated pulmonary hypertension, and maintained a flow sensitivity to preload 10 times that of constant speed control (0.39 compared with 0.04 L/min/mm Hg, respectively). Importantly, flow sensitivity to preload of the Starling-like controller depends on the gradient of the control line, and thus can be increased/decreased in a fashion similar to the heart's native inotropic response. Adaptive control of the control line gradient was simulated with a user-defined "control box" which resulted in increased LVAD flow by a total of 2.93 L/min from simulated sleep to waking activity as the control line gradient was increased from $\theta = 40$ to 50°.

Acknowledgment: Each author has contributed substantially to the research, preparation, and production of the article, and approves of its submission to the Journal. There were no ethics requirements for the research in this article.

REFERENCES

1. Birks EJ. Left ventricular assist devices. *Heart* 2010;96:63–71.
2. Salamonsen RF, Mason DG, Ayre PJ. Response of rotary blood pumps to changes in preload and afterload at a fixed speed setting are unphysiological when compared with the natural heart. *Artif Organs* 2011;35:E47–53.
3. Coats J. Wie ändern sich durch die Erregung des n. vagus die Arbeit und die innern Reize des Herzens? In: *Berichte über die Verhandlungen der Königlich Sächsischen Gesellschaft zu Leipzig*. Leipzig: Mathematisch-Physische Classe, 1869.
4. Frank O. Zur dynamik des herzmuskels. *Z Biol* 1895;32:370–437.
5. Starling EH, Visscher MB. The regulation of the energy output of the heart. *J Physiol* 1926;62:243–61.
6. Zimmer HG. Who discovered the Frank-Starling mechanism? *News Physiol Sci* 2002;17:181–4.
7. Guyton AC, Hall JE. *Textbook of Medical Physiology*, 11th Edition. Philadelphia, PA: W.B. Saunders Company, 2005.
8. Krabatsch T, Stepanenko A, Schweiger M, et al. Alternative technique for implantation of biventricular support with HeartWare implantable continuous flow pump. *ASAIO J* 2011;57:333–5.
9. Rodeheffer RJ, Gerstenblith G, Becker LC, et al. Exercise cardiac output is maintained with advancing age in healthy human subjects: cardiac dilatation and increased stroke volume compensate for a diminished heart rate. *Circulation* 1984;69:203–13.
10. Stepanoff AJ. *Centrifugal and Axial Flow Pumps*. Hoboken, NJ: John Wiley and Sons, Inc, 1957.
11. Ayre PJ, Lovell NH, Woodard JC. Non-invasive flow estimation in an implantable rotary blood pump: a study considering non-pulsatile and pulsatile flows. *Physiol Meas* 2003;24:179–89.
12. Wu Y, Allaire PE, Tao G, et al. A bridge from short-term to long-term left ventricular assist device: experimental verification of a physiological controller. *Artif Organs* 2004;28:927–32.
13. Giridharan GA, Skliar M. Physiological control of blood pumps using intrinsic pump parameters: a computer simulation study. *Artif Organs* 2006;30:301–7.
14. Moscato F, Arabia M, Colacino FM, et al. Left ventricle afterload impedance control by an axial flow ventricular assist device: a potential tool for ventricular recovery. *Artif Organs* 2010;34:736–44.
15. Gaddum NR, Timms DL, Stevens M, et al. Comparison of preload-sensitive pressure and flow controller strategies for a dual device biventricular support system. *Artif Organs* 2012; 36:256–65.
16. Noon GP, Loebe M. Current status of the MicroMed DeBakey Noon Ventricular Assist Device. *Tex Heart Inst J* 2010;37:652–3.
17. AlOmari AH, Savkin AV, Karantonis DM, Lim E, Lovell NH. Non-invasive estimation of pulsatile flow and differential pressure in an implantable rotary blood pump for heart failure patients. *Physiol Meas* 2009;30:371–86.
18. Vidakovic S, Ayre P, Woodard J, et al. Paradoxical effects of viscosity on the VentrAssist rotary blood pump. *Artif Organs* 2000;24:478–82.
19. Fritz B, Cysyk J, Newswanger R, Weiss W, Rosenberg G. Development of an inlet pressure sensor for control in a left ventricular assist device. *ASAIO J* 2010;56:180–5.
20. Gaddum NR, Timms DL, Pearcy MJ. A passively controlled biventricular support device. *Artif Organs* 2010;34:473–80.
21. Gaddum NR, Timms DL, Pearcy MJ. Optimizing the response from a passively controlled biventricular assist device. *Artif Organs* 2010;34:393–401.
22. Gregory SD, Pearcy MJ, Timms D. Passive control of a biventricular assist device with compliant inflow cannulae. *Artif Organs* 2012;36:683–90.
23. Salamonsen RF, Lim E, Gaddum N, et al. Theoretical foundations of a Starling-like controller for rotary blood pumps. *Artif Organs* 2012;36:787–96.
24. Timms D, Gregory S, Greatrex N, Pearcy M, Fraser J. A compact mock circulation loop for the in-vitro testing of cardiovascular devices. *Artif Organs* 2011;34:384–91.
25. Gaddum NR, Fraser JF, Timms DL. Increasing the transmitted flow pulse in a rotary left ventricular assist device. *Artif Organs* 2012;36:859–67.
26. Stevens M, Bradley A, Wilson S, Mason D. Evaluation of a morphological filter in mean cardiac output determination: application to left ventricular assist devices. *Med Biol Eng Comput* 2013;51:891–9.
27. Birks EJ, George RS, Hedger M, et al. Reversal of severe heart failure with a continuous-flow left ventricular assist device and pharmacological therapy: a prospective study. *Circulation* 2011;123:381–90.
28. Karantonis DM, Cloherty SL, Mason DG, et al. Automated non-invasive detection of pumping states in an implantable rotary blood pump. *Conf Proc IEEE Eng Med Biol Soc* 2006;1:5386–9.